Neuro-Oncology 14(4):405–415, 2012.
doi:10.1093/neuonc/nos005
Advance Access publication February 20, 2012

Induction of brain tumor stem cell apoptosis by FTY720: a potential therapeutic agent for glioblastoma

Adriana Estrada-Bernal, Kamalakannan Palanichamy, Abhik Ray Chaudhury, and James R. Van Brocklyn

Department of Pathology (A.E.-B., A.R.C., J.R.V.B.), and Department of Radiation Oncology (K.P.), The Ohio State University, Columbus, Ohio

FTY720 is a sphingosine analogue that down regulates expression of sphingosine-1-phosphate receptors and causes apoptosis of multiple tumor cell types, including glioma cells. This study examined the effect of FTY720 on brain tumor stem cells (BTSCs) derived from human glioblastoma (GBM) tissue. FTY720 treatment of BTSCs led to rapid inactivation of ERK MAP kinase, leading to upregulation of the BH3-only protein Bim and apoptosis. In combination with temozolomide (TMZ), the current standard chemotherapeutic agent for GBM, FTY720 synergistically induced BTSC apoptosis. FTY720 also slowed growth of intracranial xenograft tumors in nude mice and augmented the therapeutic effect of TMZ, leading to enhanced survival. Furthermore, the combination of FTY720 and TMZ decreased the invasiveness of BTSCs in mouse brains. FTY720 is known to cross the blood-brain barrier and recently received Food and Drug Administration approval for treatment of relapsing multiple sclerosis. Thus, FTY720 is an excellent potential therapeutic agent for treatment of GBM.

Keywords: FTY720, glioma, sphingosine-1-phosphate, temozolomide.

Glioblastoma (GBM), the most common primary brain tumor occurring in adults, displays aggressive growth and invasion of surrounding brain tissue, leading to a median survival time of more than 1 year. The current standard treatment, radiation and chemotherapy with the DNA alkylating agent temozolomide (TMZ), is only marginally effective. Thus, there is a great need for targeted therapies aimed at pathways that drive the malignant behavior of GBM cells.

Our group is addressing the role of the bioactive lipid sphingosine-1-phosphate (S1P), which signals through a family of G protein-coupled S1P receptors (S1PRs), in GBM. S1P is produced by the signal transduction enzyme sphingosine kinase (SphK) and regulates cell proliferation, survival, and motility.[1,2] We have shown that high expression levels of the SphK isoform SphK1 correlate with a 3-fold shorter survival of GBM patients, and that SphK1 and S1P drive proliferation, invasion, and survival of GBM cell lines and primary GBM brain tumor stem cells (BTSCs).[3–8] In agreement, a recent study confirmed and extended our observations by showing that SphK1 is upregulated in astrocytic gliomas, in comparison with adjacent normal tissue, and that SphK1 expression level correlates with the histological grade of gliomas and a decrease in patient survival with high-grade gliomas.[9] In addition, other recent studies showed that SphK1 inhibition decreases growth and invasiveness of GBM cells and GBM cell xenograft growth and vascularization in mice[10] and causes apoptosis in TMZ-resistant glioma cells.[11] Thus, the SphK/S1P/S1PR signaling axis is an excellent candidate for a pathway that drives GBM malignant behavior and for a therapeutic target for this disease.

Targeting the SphK/S1P/S1PR signaling axis as a therapeutic strategy against cancer is currently the focus of intense investigation by a number of groups.[12–17] One strategy to target this pathway is to block the action of S1P on its receptors. Thus, much attention has been paid to the sphingosine analogue FTY720, which functions by downregulating expression of S1PRs. FTY720 is phosphorylated by SphK in vivo, and FTY720-P has agonist activity at 4 of the 5 known S1PRs. Of importance, however, although S1P activation of its receptors eventually results in receptor-recycling to the cell surface, long-term

Received September 19, 2011; accepted December 30, 2011.

Corresponding Author: James R. Van Brocklyn, Department of Evolution, Ecology and Organismal Biology, 418 Aronoff Laboratory, 318 W. 12th Ave., Columbus, OH 43210 (van-brocklyn.1@osu.edu).

treatment with FTY720 causes S1PR downregulation; thus, FTY720 acts as a functional antagonist of S1PR signaling.

Of interest, numerous studies on in vitro and in vivo cancer cell models have shown potent inhibitory effects of FTY720. FTY720 causes apoptosis of several types of cancer cells, including large granular lymphocyte leukemia cells,[18] hepatocellular carcinoma cells,[19] bladder cancer cells,[20] and prostate cancer cells.[21,22] One study showed induction of apoptosis by FTY720 in 4 different glioma cell lines.[23] FTY720 treatment also enhanced sensitivity to chemotherapeutic drugs in multiple myeloma cells.[24] In addition, FTY720 may spare normal cells, because it is significantly more toxic to renal cancer cells than normal kidney tubule cells[25] and protects mature oligodendrocytes[26] and oligodendrocyte progenitors[27,28] from serum and growth factor deprivation-induced apoptosis. FTY720 has shown in vivo efficacy in numerous mouse cancer models. FTY720 has decreased tumor growth in several leukemia models[29,30] and renal,[25] pancreatic,[31] breast,[32] prostate,[33,34] lung,[35] and liver cancer models.[36]

FTY720 has also been under intense investigation as a drug to treat relapsing multiple sclerosis.[37,38] In phase III clinical trials, FTY720 was well-tolerated and showed promising efficacy,[39,40] and it was therefore approved by the Food and Drug Administration in September 2010. Because of its lipophilic nature, FTY720 crosses the blood-brain barrier and accumulates at high levels in brain tissue and cerebrospinal fluid.[37,41–43] Taken together, the demonstrated effectiveness of FTY720 against cancer cells, its ability to cross the blood-brain barrier, and the fact that it is well-tolerated in human patients makes it an excellent candidate as a potential brain tumor therapeutic.

In this study, we investigated the efficacy of FTY720 against BTSCs in vitro and in vivo in an intracranial xenograft model. BTSCs have been shown to be able to self-renew and establish new tumors in mice that resemble the original tumors and are, thus, thought to be an excellent model of GBM and crucial cells to target therapeutically. We demonstrate that FTY720 is potently pro-apoptotic for human GBM-derived BTSCs and causes decreased growth of BTSC orthotopic xenograft tumors and enhanced survival time in nude mice, both alone and in combination with TMZ.

Materials and Methods

Materials

Antibodies to pERK, ERK2, and GAPDH were from Santa Cruz Biotechnology. Antibodies to pSTAT3, STAT3, Bim, PARP, and caspases 3, 7, and 9 were from Cell Signaling Technology. FTY720 was from Cayman. TMZ was from Sigma. EGF and bFGF were from R&D Systems. Cell culture medium was from Mediatech.

Cell Culture

All GBM neurosphere cells were cultured from fresh human glioma tissue obtained following surgical resection of tumors at The Ohio State University Medical Center. Institutional review board approval for collection of tissue was obtained. Tissue was cut into small pieces and then passed several times through an 18-gauge needle and then a 21-gauge needle to achieve a single cell suspension. Cells were cultured in DMEM/F12 containing B27 without vitamin A (Invitrogen) and 20 ng/mL each of EGF and bFGF (R&D Systems). Primary spheres formed in 2–4 weeks. When spheres reached a moderate size, they were passaged by trituration with a 21-gauge needle and split at a ratio of 1:2 to 1:4.

Rat primary astrocytes were a kind gift of Dr. Chien-Liang Lin from the Department of Neuroscience at The Ohio State University. They were cultured in DMEM containing 10% fetal bovine serum.

Reverse-Transcriptase Quantitative Polymerase Chain Reaction (QPCR)

Total RNA from BTSCs was prepared using the RNase Easy Qiagen spin columns according to the manufacturer's protocol. It was ensured that the A260/280 and A260/230 ratios were more than 2.0 and more than 1.75, respectively, for all the RNA samples isolated and used for QPCR studies. For reverse-transcriptase reactions, first strand cDNA was synthesized using Superscript reverse transcriptase (Invitrogen) according to the methods of the manufacturer. cDNA corresponding to 10 ng of total RNA per gene was used for QPCR analysis. The following Taqman probes (Applied Biosystems) were used for estimating the gene expression levels: ABCG2 (Hs01053796_m1), ABCB5 (Hs00698751_m1), BIRC5 (Hs00153353_m1), BMI1 (Hs00180411_m1), BMP4 (Hs00370078_m1), CDKN2A (Hs00233365_m1), CXCR4 (Hs00607978_s1), GAPDH (Hs99999 905_m1), GFAP (Hs00909238_g1), MSI1 (Hs0015 9291_m1), NES (Hs00707120_s1), OLIG1 (Hs00744 293_s1), PTEN (Hs00829813_s1), RN18S1 (Hs 039 28990_g1), SOX2 (Hs00602736_s1), TP53 (Hs0015 3349_m1), and TUBB3 (Hs00801390_s1). Relative expression level was calculated using the $\Delta\Delta C_T$ method as described.[3]

MTT Cell Proliferation Assay

MTT reduction assay was performed using the 3-(4,5-dimethythiazol-2-yl)-2,5-diphenyl tetrazolium bromide (MTT) cell proliferation assay kit from Cayman Chemical. BTSC spheres were triturated to achieve a single cell suspension, and cells were plated in a 96-well plate at a density of 4×10^3 cells/well in 100 μL of culture medium. The following day, cells were treated with vehicle or with FTY720. Three hours before the indicated time, 10 μL of MTT reagent was added to each well and incubated at 37°C in a CO_2

environment. At the indicated times, the media were carefully removed and 100 μL of crystal-dissolving solution was added to each well. The absorbance was measured at 570 nm with use of a BMG LabTech Omega plate reader.

Western Blotting

Cells were washed and lysed in 25 mM HEPES (pH, 7.5), 150 mM NaCl, 1 mM EDTA, 1% Triton X-100, 0.1% sodium dodecylsulfate, 0.5 mM DTT, 0.5% deoxycholate, 20 mM β-glycerophosphate, 1 mM sodium orthovanadate, 1 mM PMSF, and 10 μg/mL each of aprotinin and leupeptin. Equal amounts of protein were separated by sodium dodecylsulfate–polyacramide gel electrophoresis before being transferred to nitrocellulose membranes. Membranes were blocked for 1 h at room temperature in phosphate-buffered saline (PBS) + 0.1% Tween-20 containing 5% (w/v) nonfat dry milk. Membranes were probed overnight with primary antibodies and washed 3 times with PBS and Tween for 5, 10, and 15 min, followed by incubation for 1 h at room temperature with 1:5000 horseradish peroxidase-conjugated secondary antibodies (BioRad) in blocking solution. Membranes were washed as described above, followed by incubation in Pierce Super Signal West Pico chemiluminescent substrate. For quantitation, scanned images were analyzed using LabWorks (UVP BioImaging Systems), as described elsewhere.[8]

Spheroid Invasion Assay

Spheres of GBM9 cells were embedded in Matrigel and photographed at the indicated time, as previously described.[6] Invasion was analyzed using National Institutes of Health ImageJ 1.37v software, as previously described.[44]

MGMT Promoter Methylation Analysis

Genomic DNA was extracted from BTSCs with use of the Pure Link Genomic DNA Mini kit (Invitrogen), according to the manufacturer's instructions. Bisulfite conversion was performed on 500 ng genomic DNA per sample with use of the EZ DNA Methylation Kit (Zymo Research), according to instructions. PCR was performed using primers specific for methylated versus unmethylated O6-methylguanine-DNA-methyl transferase (MGMT) promoter sequences.[45]

Tumor Formation

Animal experiments were in accord with The Ohio State University Institutional Animal Care and Use Committee (IACUC). Neurospheres were disrupted by trituration. Cells were washed 3 times in PBS and resuspended at a concentration of 66 000 cells/μL. Female athymic mice (nu/nu genotype, 5–6 weeks; Harlan Laboratories) were anesthetized by an intraperitoneal injection of a mixture consisting of ketamine (10 mg/mL) and xylazine (1 mg/mL) in PBS and fitted into a stereotactic rodent frame (David Kopf Instruments). A small incision was made just lateral to the midline and bregma exposed. A small (1.0 mm) burr hole was drilled with a #7 drill bit at AP = +1, ML = −2.5, from the bregma. A 10-μL Hamilton syringe was filled with 3 μL of the cell suspension. The syringe was lined with the drilled hole, and cells were slowly deposited at a rate of 1 μL/min in the right caudate nucleus at a depth of −3 mm from dura, for a total of 2×10^5 cells/mouse. After injecting the cells, the needle remained in place for an additional 3 min before being slowly withdrawn. The incision was sutured closed using 4-0 vicryl with an rb-1 needle. Mice were treated every day, starting on the day of the surgery, with vehicle, FTY720 (10 mg/kg) through intraperitoneal injection or TMZ (5 mg/kg) by gavage.

MRI Analysis of Xenograft Tumors

The imaging was performed using a Bruker Biospin 94/30 magnet (Bruker Biospin). The animals were anesthetized with 2% isoflurane mixed with 1 L/min carbogen (95% oxygen/5% carbon dioxide mixture). Anesthesia was maintained using 1%–1.5% isoflurane. Respiration measurements were monitored during image acquisition with use of a small animal monitoring system (Model 1025, Small Animal Instruments). Body temperature was monitored using a rectal thermometer and was maintained using water-heated bedding (9.4T).

Anesthetized mice were injected by intraperitoneal delivery with 0.5 mmol/kg Magnevist (Bayer Health Care Pharmaceuticals) Gd-DTPA contrast agent. A 2.0 cm diameter receive-only mouse brain coil was placed over the head, and the mouse bed with surface coil was placed inside a 70 mm diameter linear volume coil. Anatomic imaging was done using T2-weighted RARE imaging sequence (TR = 3500 ms, TE = 36 ms, rare factor = 8, navgs = 4). T1-weighted images were collected using a RARE-T1-weighted sequence (TR = 1200 ms, TE = 7.5, rare factor = 4, navgs = 2) ~20 min after contrast delivery. This period is required for contrast absorption and its redistribution. The acquisition parameters for both the T1- and T2-weighted multi-slice scans were as follows: FOV = 20 mm × 20 mm, slice thickness = 1.0 mm, matrix size = 256 × 256.

For experiments measuring survival time of mice, survival was taken as the time to necessity of sacrifice, as determined by animal facility veterinary staff. Significance of difference in survival times was analyzed by log-rank test using GraphPad Prism software.

Tumor volume was determined using MRI stacks and ImageJ software, as previously described.[46] The scale was adjusted by measuring the distance between 2 randomly chosen but clearly recognizable points on a slice with use of the ImageJ measurement tool. This distance was set as the scale for all images to be analyzed. With use of the freehand selection tool, the tumor was outlined creating a region of interest (ROI). The area of each ROI was calculated and then multiplied by the

slice thickness (1 mm). These values were summed to calculate the tumor volume. The data are presented in cubic millimeters.

Results

FTY720 Decreases Viability of BTSCs

FTY720 has been shown to cause apoptosis of traditional glioma cell lines grown in serum-containing medium.[23] Currently, many laboratories in the glioma field are switching to the use of glioma cells grown in neurosphere conditions, which promotes the growth of stem-like cells from human glioma tissue. Neurospheres grown in this way are thought to contain tumor stem cells and more differentiated, progenitor-like cells. Thus, although they are often referred to as BTSCs, not all of the cells are truly stem cells. Nevertheless, the neurospheres show the ability to regrow in culture from individual cells, demonstrating self-renewal, and to differentiate in multiple neural lineages. Of most importance, when injected into the brains of mice, these cells more faithfully recapitulate human gliomas both histologically and genetically,[47–50] and neurosphere cells are thus considered to be a more appropriate model of this disease than serum-cultured glioma cell lines. Furthermore, neurosphere cells have been shown to be relatively resistant to radiation and chemotherapy.[51–54] We thus wished to examine the effect of FTY720 on GBM-derived neurosphere cells to determine whether it has potential as a therapeutic agent for this disease.

We cultured cells using neurosphere conditions from human glioma tissue. For use in this study, we characterized 3 cell lines, BTSC9, 44, and 57. The original tumors from which the cells were derived were examined by a board-certified neuropathologist (A.R.C.). BTSC9 was derived from a tumor composed of highly pleomorphic neoplastic cells with hyperchromatic nuclei. Scattered mitotic figures and foci of necrosis (including geographic necrosis and microvascular proliferations) were present. Because the proliferation index was 60%, this tumor was diagnosed as GBM (WHO grade IV). BTSC44 was derived from a tumor with similar histology but had a proliferation index of 25% and was also diagnosed as GBM. BTSC57 was originally diagnosed as a high-grade astrocytoma; however, no necrosis or microvascular proliferations were identified. Deletions of both 1p and 19q loci were present. Therefore, the diagnosis was anaplastic oligoastrocytoma.

Our cells were able to reform tumor spheres from individual cells when plated at 1 cell per well (data not shown). This is a common measure of self-renewal capacity.[47] To further assess the BTSC nature of these cells, we examined them for expression of neural stem cell and neural differentiative markers with use of real-time QPCR and Western blotting. As shown in Table 1, our cell lines expressed a number of markers commonly associated with neural stem cells and BTSCs, including nestin (NES), SOX2, BMI1, and Musashi-1 (MSI1). Several of the neurosphere cells also express CD133 (Fig. 1A), which is often associated with BTSCs. Our cells also express various levels of GFAP, a marker for astrocytic differentiation, and β-III-tubulin (TUBB3), a neuronal differentiative marker (Table 1). BTSC57 grown in neurosphere conditions do not express GFAP and express low levels of β-III-tubulin; however, serum induces enhanced expression of these differentiative markers, indicating multipotentiality (Fig. 1B). Although not all markers were detected in each of our

Table 1. Relative expression of glioma-associated genes in brain tumor stem cells (BTSCs) by real-time polymerase chain reaction analysis

Gene	BTSC9	BTSC44	BTSC57	BTSC61
ABCB5	1.1	1	2.28	0.08
ABCG2	0.53	2.03	3.97	0.19
BMI1	54.6	26.4	37	7.57
BIRC5	109.1	131.6	113	26.9
BMP4	19.83	0.01	ND	10.3
CDKN2A	ND	ND	ND	ND
CXCR4	0.12	5.8	35	0.05
GFAP	0.01	43.4	4.35	0.18
MSI1	4.41	20.1	17.5	ND
NES	0.95	292	445.7	1.45
OLIG1	0.08	0.72	0.35	0.04
PTEN	0.26	ND	ND	0.03
SOX2	ND	13.8	12.5	0.04
TUBB3	18.9	160.9	109.1	18.4
TERT	0.04	0.1	0.09	0.03
TP53	55.3	117.8	111.4	25.5

Abbreviations: ND, not detected.

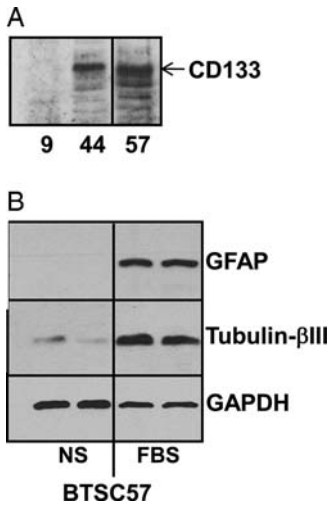

Fig. 1. Partial characterization of brain tumor stem cells (BTSCs). (A) Lysates of the indicated BTSCs were immunoblotted with antibodies specific for CD133. (B) BTSC57 cells were cultured in defined neurosphere medium (NS) or in medium containing 10% FBS. Lysates were blotted for differentiative markers. Longer exposures revealed very low-level GFAP expression in cells grown in neurosphere medium.

cell lines, our cell lines maintained their self-renewal capacity (i.e., when plated as single cells and maintained in optimal conditions for propagation and prevention of differentiation, we obtained neurospheres that were capable of generating tumors).

We also found that many of our neurosphere lines were negative for expression of the tumor suppressor genes PTEN and p16 (CDKN2A), which are commonly deleted in GBM. The exception was BTSC9 cells, which do express PTEN. Sequencing of PCR-amplified PTEN from BTSC9 cDNA revealed that these cells express wild-type PTEN (data not shown). However, BTSC9 cells do express the constitutively active EGFR receptor mutant EGFRvIII.[8] In addition, we determined that BTSC9 cells retain expression of EGFRvIII for at least 15 passages.[8] This is significant, because serum-cultured glioma cells commonly lose overexpression of EGFR. Thus, our neurosphere lines have common mutations seen in GBM, express several neural stem cell markers, have the potential to differentiate toward multiple neural lineages, and form tumors resembling GBM in nude mice brains.[8] Therefore, although the neurospheres likely contain tumor stem-like cells and at least partially differentiated tumor cells, they represent an appropriate model of GBM for this study, and we will refer to them as BTSCs.

Next, we assessed the potential effectiveness of FTY720 against BTSCs. As shown in Fig. 2A, FTY720 dramatically decreased the number of viable cells in 4 different BTSC lines tested. BTSC9 was the most sensitive to FTY720; however, all 4 cell lines showed significantly decreased viability in the presence of FTY720 at concentrations as low as 1 μg/mL. At 4 μg/mL, FTY720 completely killed BTSC9 cells, clearly indicating that the tumor stem cells and any more differentiated cells within these spheres were killed. As shown in Fig. 2B, FTY720 was much less toxic to primary astrocytes, with no effect on astrocyte viability up to 4 μg/mL. Toxicity of FTY720 for primary astrocytes was detected at 10 μg/mL, approximately 1 order of magnitude higher than for BTSCs.

We also measured the levels of S1PRs, which are targeted by FTY720, in 2 of our BTSC lines. Both BTSC9 and BTSC57 expressed S1PR1, 2, and 3, with BTSC57 expressing the higher levels of these 3 receptors (Fig. 2C). It is possible that the lower level of S1PR expression in BTSC9 renders them more sensitive to FTY720, because BTSC57 might require more of the drug to overcome S1PR signaling. Thus, BTSC9 were primarily used for further experimentation.

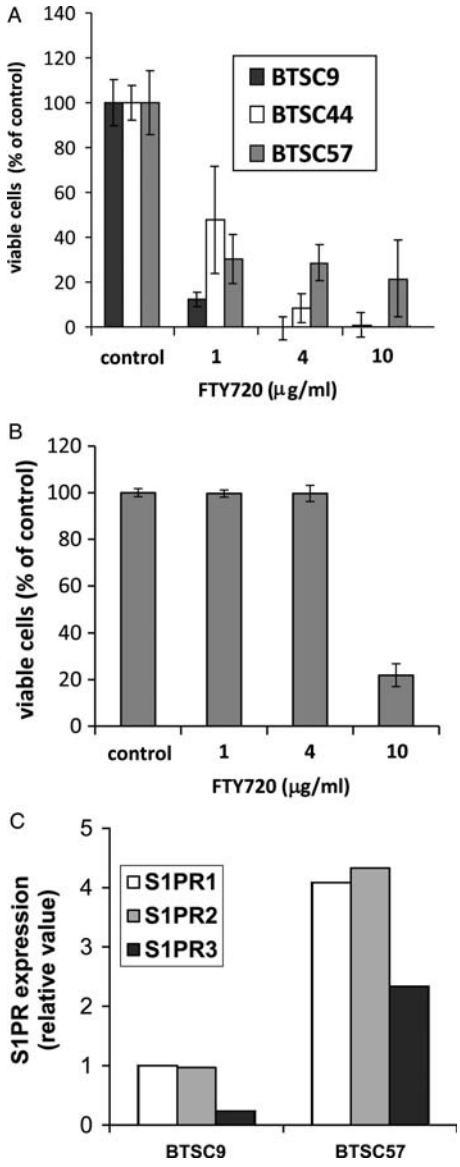

Fig. 2. Induction of apoptosis in brain tumor stem cells (BTSCs) by FTY720. (A) Three different BTSC lines were treated with FTY720 for 4 h at the indicated concentrations. Proliferation was measured using either an MTT assay or WST-1 assay according to instructions. Data are means ± standard deviations of triplicate samples. All FTY720 treatments were statistically significantly different from control by Student's t test ($P < .05$). Three independent experiments provided similar results. (B) Rat primary astrocytes were treated with the indicated concentrations of FTY720, and viable cells were measured by WST-1 assay. (C) Expression of S1P receptors was examined in BTSC9 and BTSC57 cells using quantitative real-time polymerase chain reaction analysis.

Induction of Apoptotic Signaling by FTY720 in BTSCs

To examine the mechanism of FTY720-induced toxicity in BTSCs, we treated BTSC9 cells with FTY720 and examined the effects on mitogenic and apoptotic signaling pathways. As shown in Fig. 3A, FTY720 treatment of BTSC9 cells leads to rapid inactivation of ERK MAP kinase. Levels of phospho-ERK were decreased to 0.11 of the control by 15 min, and phospho-ERK was undetectable by 3 h after FTY720 treatment (Table 2). Subsequently, a potent upregulation of the BH3-only protein Bim was seen, with a 1.8-fold increase at 15 min and a peak of a 15.3-fold increase at 2 h. Bim is well-established to activate apoptosis through the intrinsic mitochondrial pathway.[55] In agreement, at later times, cleavage of caspase-9 and the executioner caspase-7 occurred.

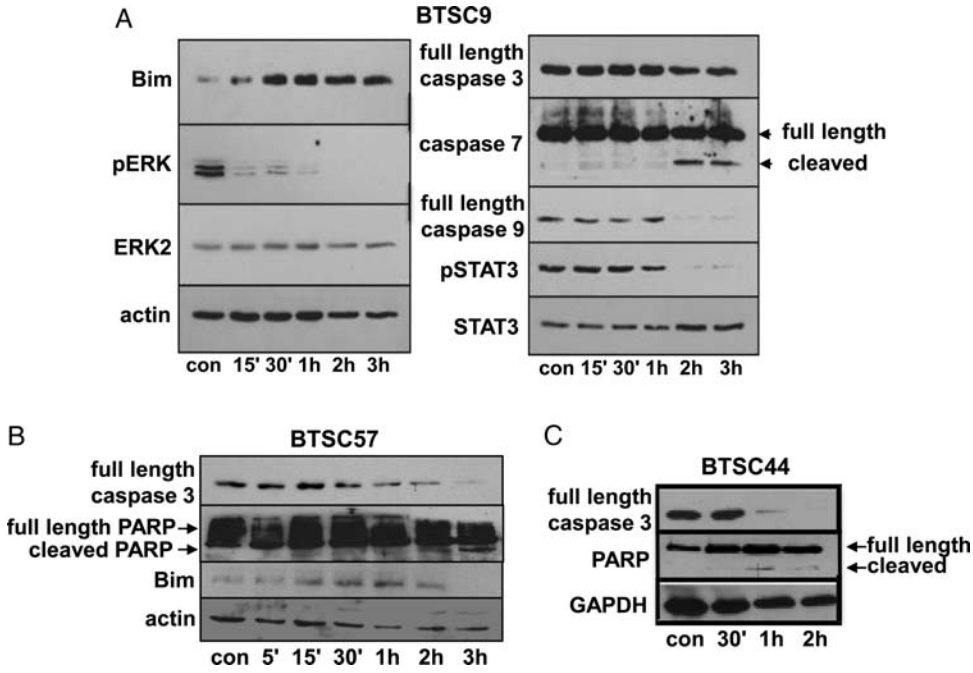

Fig. 3. Effect of FTY720 on pro- and anti-apoptotic proteins in brain tumor stem cells (BTSCs). BTSC9 (A), BTSC57 (B), or BTSC44 (C) cells were treated with vehicle alone for 3 h (con) or 4 μg/mL FTY720 for the indicated time, and cell lysates were immunoblotted for regulators of apoptosis. Two independent experiments provided similar results.

Table 2. Quantitation of Western blots of BTSC9 lysates shown in Fig. 3A

	pERK	pSTAT3	Bim	Casp 3	Casp 9	$Casp7_{fl}$	$Casp7_{fr}$
con	1	1	1	1	1	1	0
15′	0.11	1.15	1.8	0.78	0.6	0.83	0
30′	0.12	1.05	6.4	1.01	0.5	0.92	0
1 h	0.04	0.70	5.7	0.75	0.8	0.61	0
2 h	0.03	0.04	15.3	1.02	0	1.93	0.5
3 h	0	0.07	7.2	0.86	0.1	1.08	0.3

pERK and pSTAT3 were quantitated relative to the respective unphosphorylated proteins. All others were quantitated relative to actin loading control.
Abbreviations: fl, full length; fr, fragment.

This mechanism works similarly in other BTSC lines. Bim was also upregulated in response to FTY720 in BTSC57 (Fig. 3B), peaking at 1 h with a 32.5-fold increase. In this line, we saw cleavage of caspase-3. Caspase-3 was also cleaved in FTY720-treated BTSC44 cells (Fig. 3C). In both BTSC57 and BTSC44, we also saw the appearance of cleaved PARP at later times, indicating apoptosis. Thus, in several BTSC lines, FTY720 leads to apoptosis, and this response is likely to be downstream of a rapid inactivation of ERK, leading to upregulation of Bim and activation of the mitochondrial death pathway.

We also saw decreased phosphorylation of STAT3 at Tyr705 in response to FTY720 (Fig. 3A). This is an intriguing effect of FTY720; however, it occurred at later times than ERK inactivation and Bim upregulation, showing a 30% decrease at 1 h FTY720 treatment. Thus, STAT3 inactivation is unlikely to be the primary inducer of apoptosis. However, it remains possible that STAT3 inactivation might contribute to the apoptotic response to FTY720 in the BTSCs at a later time.

Effect of FTY720 on BTSC Invasiveness

Invasion of GBM cells is an important aspect of malignant behavior, commonly leading to tumor recurrence and patient mortality. To assess the effect of FTY720 on invasiveness of BTSCs, we used a spheroid invasion assay in which spheres of BTSCs were embedded within a collagen matrix and photographed over time as cells invade into the matrix. By 4 days of culture, BTSC9 cells invaded extensively under control conditions; however, invasion was almost completely inhibited by treatment with 1 μg/mL FTY720 (Fig. 4). It should be noted that the decreased invasion was seen at similar concentrations to those that caused apoptosis (Fig. 2). Thus, it is unclear whether this is a specific effect of invasiveness or merely a result of toxicity.

Combination of FTY720 with TMZ

The current standard therapy for patients with GBM involves radiation therapy and treatment with the DNA alkylating drug TMZ. Although addition of TMZ extends survival among patients with GBM by a few months on average, it is ineffective in the long term. In addition, clinical trials with more targeted therapeutics, including EGFR inhibitors, have been largely

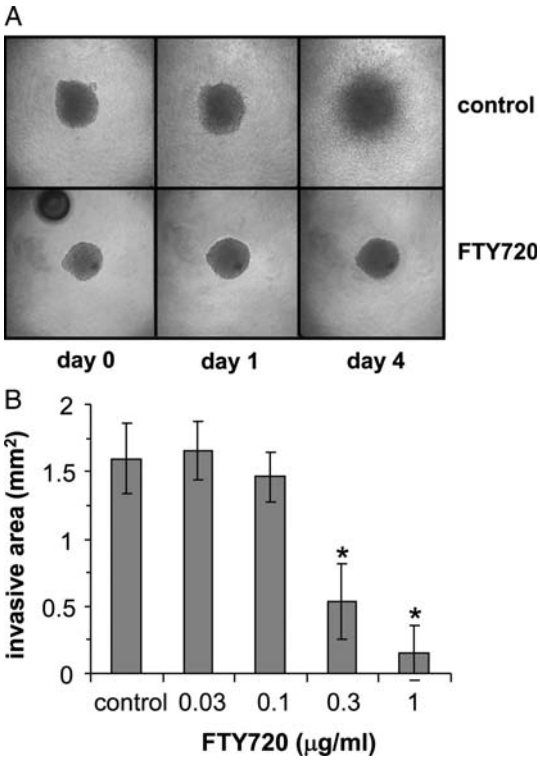

Fig. 4. Effect of FTY720 on brain tumor stem cell (BTSC) invasiveness. (A) BTSC9 tumor spheres were embedded in a collagen matrix in the presence of 1 μg/mL FTY720 or vehicle (control). Cells invading into the collagen were photographed at the indicated times. (B) After 4 days in the presence of vehicle (control) or of the indicated concentration of FTY720, the area of invasion into collagen was quantitated using the National Institutes of Health ImageJ software. Data are means ± standard deviations from triplicate wells. *Statistically significant difference by Student's *t* test ($P < .01$).

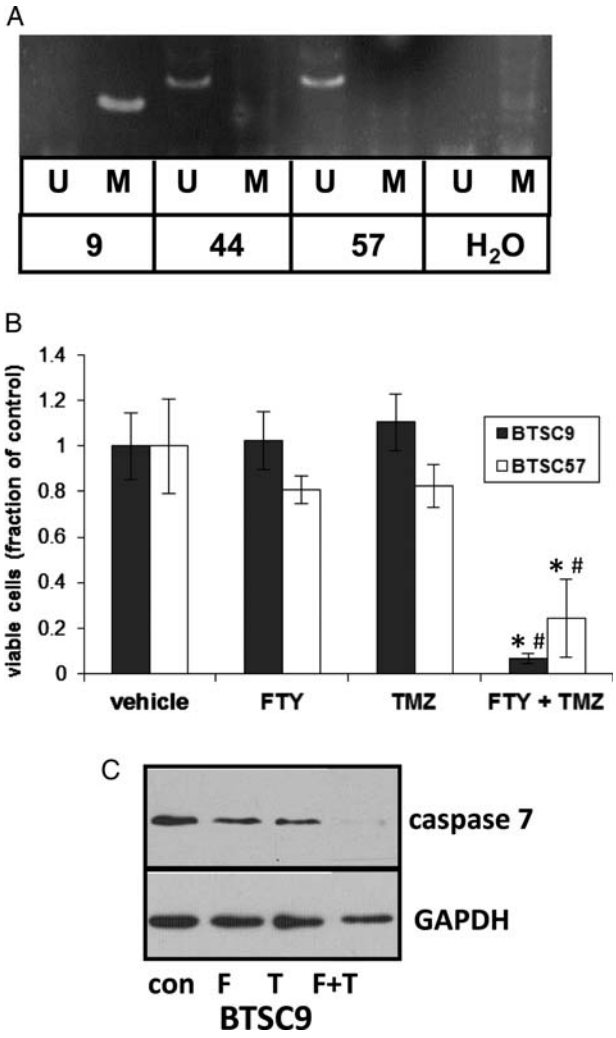

Fig. 5. Combination of FTY720 with TMZ. (A) MGMT promoter methylation was examined using methylation-specific polymerase chain reaction (U = unmethylated, M = methylated). (B) BTSC9 or BTSC57 were treated with 0.03 μg/mL of FTY720 or 10 μM of TMZ separately or in combination, and after 4 days, viability was measured by MTT assay. Data are means ± standard deviations from triplicate samples. *Statistically significant difference from FTY720 alone. #Statistically significant difference from TMZ alone by Student's *t* test. (C) BTSC9 were treated with FTY720 (F) or TMZ (T) at the concentrations listed above separately or in combinations, and lysates were immunoblotted for full-length caspase 7 or GAPDH.

unsuccessful, and the prevailing opinion in the field is that effective GBM therapy will eventually require treatment with multiple drugs. To begin to assess the effectiveness of FTY720 in combination with other drugs, we examined its effects in the presence of TMZ. TMZ is known to be more effective against GBM tumors with methylation of the O^6-methylguanine DNA methyltransferase (MGMT) promoter. Decreased expression of MGMT in these cells prevents the repair of DNA damage done by TMZ, rendering cells more sensitive to TMZ. BTSC9 cells have MGMT promoter methylation, whereas BTSC44 and BTSC57 do not, as determined by methylation-specific PCR (Fig. 5A). We therefore examined the effect of FTY720 on BTSC9 and BTSC57 cells in the presence of TMZ. Figure 5B shows that a low concentration of FTY720 (0.03 μg/mL), which does not affect BTSC9 cell viability alone, has a potent toxic effect on BTSC9 cells in combination with TMZ. Combination index (CI) analysis[56] of these data revealed a CI of 0.2, indicating a synergistic effect. A similar effect was seen for FTY720 and TMZ toxicity for BTSC57, although these cells do not possess MGMT promoter methylation. This study shows that FTY20 exhibits synergistic toxicity when administered with TMZ, irrespective of MGMT status. Furthermore, in BTSC9, cleavage of the executioner caspase-7 was dramatically enhanced by 0.03 μg/mL of FTY720 plus TMZ, in comparison with either drug alone (Fig. 5C). Quantitation of the Western blot shown in Fig. 5C revealed that caspase 7 decreased to 0.51 and 0.43 of the control due to FTY720 and TMZ, respectively, and to 0.21 of the control due to the combination of the 2 drugs.

Effect of FTY720 on GBM BTSCs In Vivo

To evaluate the effectiveness of FTY720 on BTSCs in vivo, we used orthotopic xenografts in nude mice brains. We previously showed that BTSC9 cells form tumors in mouse brains that resemble GBM histologically, as determined by a board-certified neuropathologist (A.R.C.), with high cellularity, multiple mitotic figures, diffuse invasiveness, and focal areas of necrosis.[8] In our experience, tumors formed from these cells lead to death of mice within approximately 2 weeks following injection.

Mice were injected orthotopically with BTSC9 cells and subsequently treated with vehicle alone, FTY720, TMZ, or both drugs in combination. Eleven days after injection, tumors were assessed by MRI, and tumor size was measured on serial images to determine volume. As shown in Fig. 6A and B, treatment with FTY720 led to a 50% reduction in tumor volume seen on the MRI. TMZ was more effective, decreasing tumor volume to approximately 25% of the control. FTY720 plus TMZ showed an effect similar to TMZ alone at this time.

Survival time of mice was also determined. FTY720 alone significantly increased survival over control ($P = .0069$) (Fig. 6C). TMZ alone also increased survival time; however, mice treated with FTY720 plus TMZ survived longest. Survival with FTY720 plus TMZ was significantly different from either drug alone ($P = .0062$ vs. FTY720 alone, and $P = .0347$ vs. TMZ alone). The increase in median survival of various treatment arms, such as FTY20, TMZ, and FTY20 + TMZ, were found to be 7%, 35%, and 57%, respectively. Furthermore, histological analysis revealed that tumors from control, FTY720-treated, and TMZ-treated mice showed a diffuse border, with numerous cells invading beyond the tumor mass. In contrast, in mice treated with both FTY720 and TMZ, the tumors were more circumscribed, and fewer invading cells were seen (Fig. 6D). Thus, FTY720 is effective against our GBM model alone and in combination with TMZ, decreasing tumor growth and increasing survival time.

Discussion

In this article, we show that FTY720 has potential as a therapeutic agent for GBM on the basis of several findings. First, FTY720 is a remarkably potent inducer of apoptosis for BTSCs. Second, FTY720 acts synergistically with TMZ, a current standard drug used for GBM, to induce apoptosis of BTSCs. Third, FTY720 increased survival in a rodent model of GBM, both alone and in combination with TMZ. Fourth, FTY720 plus TMZ decreased invasiveness of xenografted BTSCs in nude mouse brains. In addition, FTY720 recently received Food and Drug Administration approval for treatment of relapsing multiple sclerosis and, thus, has been shown to be well-tolerated in human patients and to enter the central nervous system.

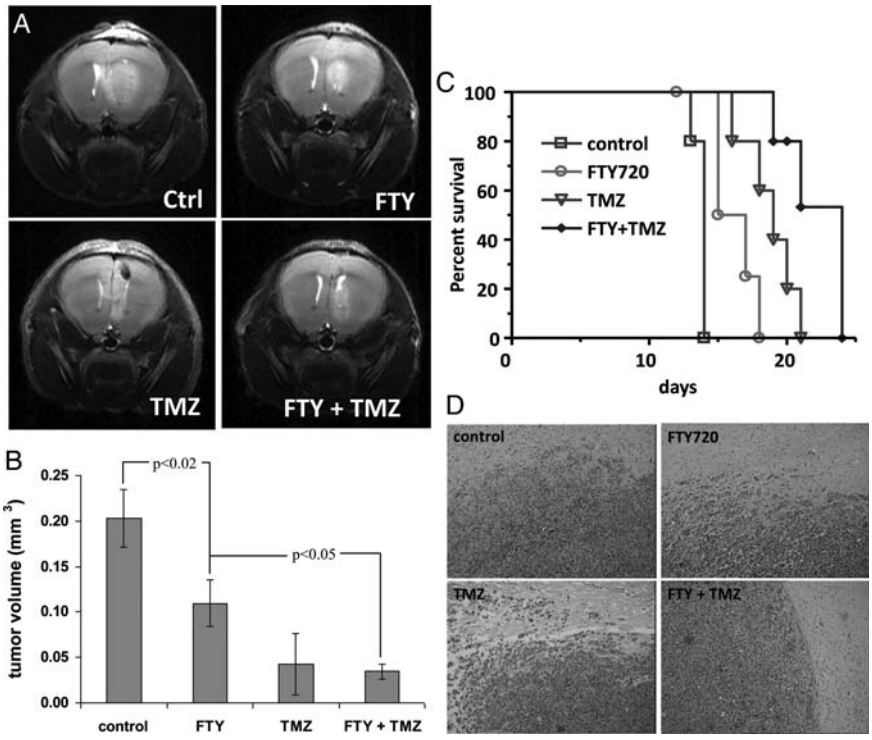

Fig. 6. Combined FTY720 with TMZ in vivo. (A) Representative MRI of tumors in mice with BTSC9 intracranial xenografts 11 days following injection of cells. Mice were treated with vehicle (control), 10 mg/kg FTY720, 5 mg/kg TMZ, or both. (B) Tumor volume was measured as described in Materials and Methods. Data are means ± standard deviations from 3 mice per group. (C) Survival analysis of mice treated as in panel A (5 mice per group). (D) H & E sections showing lack of invasion and well circumscribed tumors in mice treated with FTY720 plus TMZ, compared with control mice or mice treated with either drug alone.

The effectiveness of FTY720 against BTSCs is particularly interesting, because BTSCs have been shown to be resistant to both chemotherapy and radiation therapy.[51–54] Moreover, BTSCs are thought to represent the cells that are capable of repopulating tumors because of their ability to self-renew and, thus, should be necessary for the recurrence of tumors following surgical resection, which inevitably leads to death in patients with GBM. Thus, targeting BTSCs therapeutically would be critical to prevent recurrence of tumors following surgery and chemotherapy.

The mechanism of FTY720 induction of apoptosis in BTSCs appears to be through activation of the intrinsic mitochondrial death pathway. This is evidenced by the rapid accumulation of the BH3-only protein Bim, leading to caspase-9 and eventually casapase-7 or caspase-3 activation. Phosphorylation of Bim by ERK MAP kinase leads to its degradation, and thus, ERK inactivation can cause Bim accumulation.[57,58] In agreement, we found rapid and potent ERK inactivation following FTY720 treatment. Other studies have shown that FTY720 can cause ERK inactivation through activation of protein phosphatase 2A (PP2A). However, neither okadaic acid, which inhibits PP2A, nor tautomycin, which inhibits PP1, was able to prevent ERK inactivation or apoptosis in response to FTY720 in our BTSCs (data not shown).

FTY720 is also well-known for targeting S1P receptors leading to receptor degradation. Although we have seen effects of FTY720 on the $S1PR_1$ receptor in BTSCs, $S1PR_1$ degradation occurs at a later time than ERK inactivation and Bim upregulation (data not shown), suggesting that this is not the initiating event in FTY720-induced apoptosis of BTSCs. Furthermore, FTY720 has been shown to inhibit SphK1;[59] however, in our BTSCs, no inhibition of SphK1 activity was seen (data not shown). Thus, although modulation of S1P signaling may be involved in the effects of FTY720 on BTSCs, the initial target for FTY720 that leads to ERK inactivation and eventual apoptosis is unknown at this time.

Although FTY720 was effective in our mouse xenograft model, it was not as effective as one would have predicted on the basis of the in vitro potency of the drug against BTSCs. Tumor growth was significantly slowed by FTY720, and mouse survival was extended, though only modestly. It is currently unclear why FTY720 does not appear to affect BTSCs in vivo as potently as in vitro; several possibilities exist. First, it is possible that FTY720 does not accumulate in the brain at a high enough concentration to kill BTSCs. This would seem unlikely, because 2 separate studies demonstrated that FTY720 enters and accumulates in brain tissue at concentrations similar to those used in our in vitro studies.[41,42] It should be noted that, although some studies have administered FTY720 to mice by gavage and others by intraperitoneal injection, both methods of delivery had similar effects in our experiments (data not shown).

Another possibility is that FTY720 becomes highly phosphorylated in nude mice, resulting in too low levels of unphosphorylated FTY720 in the brain. FTY720-P has been shown to be ineffective at killing cancer cells,[60,61] and this may therefore prevent toxicity against BTSCs. In agreement, FTY720-P was much less effective at inducing apoptosis of BTSCs in our study (data not shown). If FTY720 phosphorylation is the reason for its lower than expected efficacy in vivo, nonphosphorylatable analogues might prove to be more effective and could also have the added benefit of decreasing potential immunosuppressive effects of FTY720 in patients with glioma, as has been shown for hepatocellular carcinoma.[62]

A third possibility is that FTY720 may accumulate in white matter tracts in the brain,[41] thus sequestering it from the xenografted BTSCs. Experiments examining the accumulation and phosphorylation state of FTY720 in our model will shed light on these possibilities.

Although FTY720 alone blocked in vitro invasion of BTSC9 cells, this response required concentrations of the drug that were toxic for BTSCs; thus, it is unclear whether the decreased invasiveness seen in this assay is a result of the toxicity. However, FTY720 in combination with TMZ appeared to decrease invasiveness of BTSCs in our xenograft model. Invasion is an important aspect of GBM malignancy, because these tumors are diffusely invasive, leading to inevitable recurrence and patient mortality following resection. It is likely that inhibition of invasion would be more therapeutically significant in human patients than in a mouse model, where a rapidly growing tumor in the small mouse brain will likely kill the animal very quickly, regardless of the invasiveness of the cells. Additional work is necessary to determine whether the effect of FTY720 is a specific effect on the invasion process or merely a reflection of increased toxicity of the drug combination for tumor cells.

In addition, it will be interesting to determine the genetic profile of GBM tumors that respond best to FTY720. Of the BTSC lines examined in this study, FTY720 was the most potent against BTSC9. This cell line expresses the EGFRvIII mutant and wild-type PTEN. However, FTY720 also killed several other BTSC lines that do not express EGFRvIII and are negative for PTEN expression. Furthermore, FTY720 was also effective against BTSC57, which expressed higher levels of S1PR and CD133. Although the significance of CD133 is somewhat controversial, it has been widely used as a stem cell marker in GBMs. Therefore, FTY720 could be an effective way of targeting $CD133^+$ cells. Thus, it is possible that FTY720 may affect BTSCs with disparate expression profiles. Further understanding of the mechanism of action of FTY720 against BTSCs and characterization of additional BTSC lines will shed more light on this. In summary, we have identified FTY720 as a potential therapeutic agent for GBM that may be very effective against BTSCs. Additional studies are needed to determine the optimum dosing regimen, combinations with other therapeutics, and responsiveness of cases with various mutational profiles, as well as further defining the mechanism of action of this drug.

Acknowledgments

We thank Dr. Chien-Liang "Glenn" Lin for his generous gift of rat primary astrocytes.

Conflict of interest statement. None declared.

Funding

This work was supported by the National Cancer Institute (R21CA124685 to J.R.V.B.) and the Department of Pathology, The Ohio State University. MRI was performed by the Small Animal Imaging Shared Resource supported by National Institutes of Health (CA016058).

References

1. Spiegel S, Milstien S. Sphingosine-1-phosphate: an enigmatic signalling lipid. *Nat Rev Mol Cell Biol*. 2003;4:397–407.
2. Maceyka M, Payne SG, Milstien S, Spiegel S. Sphingosine kinase, sphingosine-1-phosphate, and apoptosis. *Biochim Biophys Acta*. 2002;1585:193–201.
3. Van Brocklyn JR, Jackson CA, Pearl DK, Kotur MS, Snyder PJ, Prior TW. Sphingosine kinase-1 expression correlates with poor survival of patients with glioblastoma multiforme. Roles of sphingosine kinase isoforms in growth of glioblastoma cell lines. *J Neuropathol Exp Neurol*. 2005;64:695–705.
4. Van Brocklyn JR, Letterle CA, Snyder PJ, Prior TW. Sphingosine-1-phosphate stimulates human glioma cell proliferation through G_i-coupled receptors: Role of ERK MAP kinase and phosphatidylinositol 3-kinase β. *Cancer Lett*. 2002;181:195–204.
5. Van Brocklyn JR, Young N, Roof R. Sphingosine-1-phosphate stimulates motility and invasiveness of human glioblastoma multiforme cells. *Cancer Lett*. 2003;199:53–60.
6. Young N, Pearl DK, Van Brocklyn JR. Sphingosine-1-phosphate regulates glioblastoma cell invasiveness through the urokinase plasminogen activator system and CCN1/Cyr61. *Mol Cancer Res*. 2009;7:23–32.
7. Young N, Van Brocklyn JR. Roles of sphingosine-1-phosphate (S1P) receptors in malignant behavior of glioma cells. Differential effects of $S1P_2$ on cell migration and invasiveness. *Exp Cell Res*. 2007;313:1615–1627.
8. Estrada-Bernal A, Lawler SE, Nowicki MO, Ray Chaudhury A, Van Brocklyn JR. The role of sphingosine kinase-1 in EGFRvIII-regulated growth and survival of glioblastoma cells. *J Neuro-Oncol*. 2011;102:353–366.
9. Li J, Guan HY, Gong LY, et al. Clinical significance of sphingosine kinase-1 expression in human astrocytomas progression and overall patient survival. *Clin Cancer Res*. 2008;14:6996–7003.
10. Kapitonov D, Allegood JC, Mitchell C, et al. Targeting sphingosine kinase 1 inhibits Akt signaling, induces apoptosis, and suppresses growth of human glioblastoma cells and xenografts. *Cancer Res*. 2009;69:6915–6923.
11. Bektas M, Johnson SP, Poe WE, Bigner DD, Friedman HS. A sphingosine kinase inhibitor induces cell death in temozolomide resistant glioblastoma cells. *Cancer Chemother Pharmacol*. 2009;64:1053–1058.
12. Sabbadini RA. Targeting sphingosine-1-phosphate for cancer therapy. *Br J Cancer*. 2006;95:1131–1135.
13. Murph M, Mills GB. Targeting the lipids LPA and S1P and their signalling pathways to inhibit tumour progression. *Expert Rev Mol Med*. 2007;9:1–18.
14. Huwiler A, Zangemeister-Wittke U. Targeting the conversion of ceramide to sphingosine 1-phosphate as a novel strategy for cancer therapy. *Crit Rev Oncol Hematol*. 2007;63:150–159.
15. Shida D, Takabe K, Kapitonov D, Milstien S, Spiegel S. Targeting SphK1 as a new strategy against cancer. *Curr Drug Targets*. 2008;9:662–673.
16. Cuvillier O. Downregulating sphingosine kinase-1 for cancer therapy. *Expert Opin Ther Targets*. 2008;12:1009–1020.
17. Saddoughi SA, Song P, Ogretmen B. Roles of bioactive sphingolipids in cancer biology and therapeutics. *Subcell Biochem*. 2008;49:413–440.
18. Shah MV, Zhang R, Irby R, et al. Molecular profiling of LGL leukemia reveals role of sphingolipid signaling in survival of cytotoxic lymphocytes. *Blood*. 2008;112:770–781.
19. Hung JH, Lu YS, Wang YC, et al. FTY720 induces apoptosis in hepatocellular carcinoma cells through activation of protein kinase Cd signaling. *Cancer Res*. 2008;68:1204–1212.
20. Azuma H, Takahara S, Horie S, Muto S, Otsuki Y, Katsuoka Y. Induction of apoptosis in human bladder cancer cells in vitro and in vivo caused by FTY720 treatment. *J Urol*. 2003;169:2372–2377.
21. Wang JD, Takahara S, Nonomura N, et al. Early induction of apoptosis in androgen-independent prostate cancer cell line by FTY720 requires caspase-3 activation. *Prostate*. 1999;40:50–55.
22. Permpongkosol S, Wang JD, Takahara S, et al. Anticarcinogenic effect of FTY720 in human prostate carcinoma DU145 cells: modulation of mitogenic signaling, FAK, cell-cycle entry and apoptosis. *Int J Cancer*. 2002;98:167–172.
23. Sonoda Y, Yamamoto D, Sakurai S, et al. FTY720, a novel immunosuppressive agent, induces apoptosis in human glioma cells. *Biochem Biophys Res Commun*. 2001;281:282–288.
24. Yasui H, Hideshima T, Raje N, et al. FTY720 induces apoptosis in multiple myeloma cells and overcomes drug resistance. *Cancer Res*. 2005;65:7478–7484.
25. Ubai T, Azuma H, Kotake Y, et al. FTY720 induced Bcl-associated and Fas-independent apoptosis in human renal cancer cells in vitro and significantly reduced in vivo tumor growth in mouse xenograft. *Anticancer Res*. 2007;27:75–88.
26. Miron VE, Hall JA, Kennedy TE, Soliven B, Antel JP. Cyclical and dose-dependent responses of adult human mature oligodendrocytes to fingolimod. *Am J Pathol*. 2008;173:1143–1152.
27. Coelho RP, Payne SG, Bittman R, Spiegel S, Sato-Bigbee C. The immunomodulator FTY720 has a direct cytoprotective effect in oligodendrocyte progenitors. *J Pharmacol Exp Ther*. 2007;323:626–635.
28. Miron VE, Jung CG, Kim HJ, Kennedy TE, Soliven B, Antel JP. FTY720 modulates human oligodendrocyte progenitor process extension and survival. *Ann Neurol*. 2008;63:61–71.
29. Liu Q, Zhao X, Frissora F, et al. FTY720 demonstrates promising preclinical activity for chronic lymphocytic leukemia and lymphoblastic leukemia/lymphoma. *Blood*. 2008;111:275–284.
30. Neviani P, Santhanam R, Oaks JJ, et al. FTY720, a new alternative for treating blast crisis chronic myelogenous leukemia and Philadelphia chromosome-positive acute lymphocytic leukemia. *J Clin Invest*. 2007;117:2408–2421.

31. Shen Y, Wang X, Xia W, et al. Antiproliferative and overadditive effects of rapamycin and FTY720 in pancreatic cancer cells in vitro. *Transplant Proc*. 2008;40:1727–1733.
32. Azuma H, Horie S, Muto S, et al. Selective cancer cell apoptosis induced by FTY720; evidence for a Bcl-dependent pathway and impairment in ERK activity. *Anticancer Res*. 2003;23:3183–3193.
33. Chua CW, Lee DT, Ling MT, et al. FTY720, a fungus metabolite, inhibits in vivo growth of androgen-independent prostate cancer. *Int J Cancer*. 2005;117:1039–1048.
34. Zhou C, Ling MT, Kin-Wah Lee T, Man K, Wang X, Wong YC. FTY720, a fungus metabolite, inhibits invasion ability of androgen-independent prostate cancer cells through inactivation of RhoA-GTPase. *Cancer Lett*. 2006;233:36–47.
35. Salinas NR, Lopes CT, Palma PV, Oshima CT, Bueno V. Lung tumor development in the presence of sphingosine 1-phosphate agonist FTY720. *Pathol Oncol Res*. 2009;15:549–554.
36. Ng KT, Man K, Ho JW, et al. Marked suppression of tumor growth by FTY720 in a rat liver tumor model: the significance of down-regulation of cell survival Akt pathway. *Int J Oncol*. 2007;30:375–380.
37. Brinkmann V. FTY720 (fingolimod) in multiple sclerosis: therapeutic effects in the immune and the central nervous system. *Br J Pharmacol*. 2009;158:1173–1182.
38. Chun J, Hartung HP. Mechanism of action of oral fingolimod (FTY720) in multiple sclerosis. *Clin Neuropharmacol*. 2010;33:91–101.
39. Kappos L, Radue EW, O'Connor P, et al. A placebo-controlled trial of oral fingolimod in relapsing multiple sclerosis. *N Engl J Med*. 2010;362:387–401.
40. Cohen JA, Barkhof F, Comi G, et al. Oral fingolimod or intramuscular interferon for relapsing multiple sclerosis. *N Engl J Med*. 2010;362:402–415.
41. Foster CA, Howard LM, Schweitzer A, et al. Brain penetration of the oral immunomodulatory drug FTY720 and its phosphorylation in the central nervous system during experimental autoimmune encephalomyelitis: consequences for mode of action in multiple sclerosis. *J Pharmacol Exp Ther*. 2007;323:469–475.
42. Meno-Tetang GM, Li H, Mis S, et al. Physiologically based pharmacokinetic modeling of FTY720 (2-amino-2[2-(-4-octylphenyl)ethyl] propane-1,3-diol hydrochloride) in rats following oral and intravenous doses. *Drug Metab Dispos*. 2006;34:1480–1487.
43. Miron VE, Schubart A, Antel JP. Central nervous system-directed effects of FTY720 (fingolimod). *J Neurol Sci*. 2008;274:13–17.
44. Stein AM, Demuth T, Mobley D, Berens M, Sander LM. A mathematical model of glioblastoma tumor spheroid invasion in a three-dimensional in vitro experiment. *Biophys J*. 2007;92:356–365.
45. Esteller M, Hamilton SR, Burger PC, Baylin SB, Herman JG. Inactivation of the DNA repair gene O^6-methylguanine-DNA methyltransferase by promoter hypermethylation is a common event in primary human neoplasia. *Cancer Res*. 1999;59:793–797.
46. Dello SA, van Dam RM, Slangen JJ, et al. Liver volumetry plug and play: do it yourself with ImageJ. *World J Surg*. 2007;31:2215–2221.
47. Singh SK, Hawkins C, Clarke ID, et al. Identification of human brain tumour initiating cells. *Nature*. 2004;432:396–401.
48. Yuan X, Curtin J, Xiong Y, et al. Isolation of cancer stem cells from adult glioblastoma multiforme. *Oncogene*. 2004;23:9392–9400.
49. Galli R, Binda E, Orfanelli U, et al. Isolation and characterization of tumorigenic, stem-like neural precursors from human glioblastoma. *Cancer Res*. 2004;64:7011–7021.
50. Lee J, Kotliarova S, Kotliarov Y, et al. Tumor stem cells derived from glioblastomas cultured in bFGF and EGF more closely mirror the phenotype and genotype of primary tumors than do serum-cultured cell lines. *Cancer Cell*. 2006;9:391–403.
51. Bao S, Wu Q, McLendon RE, et al. Glioma stem cells promote radioresistance by preferential activation of the DNA damage response. *Nature*. 2006;444:756–760.
52. Liu G, Yuan X, Zeng Z, et al. Analysis of gene expression and chemoresistance of $CD133^+$ cancer stem cells in glioblastoma. *Mol Cancer*. 2006;5:67. doi: 10.1186/1476-4598-1185-1167.
53. Johannessen TC, Bjerkvig R, Tysnes BB. DNA repair and cancer stem-like cells - Potential partners in glioma drug resistance? *Cancer Treat Rev*. 2008;34:558–567.
54. Ma S, Lee TK, Zheng BJ, Chan KW, Guan XY. CD133+ HCC cancer stem cells confer chemoresistance by preferential expression of the Akt/PKB survival pathway. *Oncogene*. 2008;27:1749–1758.
55. Gillings AS, Balmanno K, Wiggins CM, Johnson M, Cook SJ. Apoptosis and autophagy: BIM as a mediator of tumour cell death in response to oncogene-targeted therapeutics. *FEBS J*. 2009;276:6050–6062.
56. Chou TC. Theoretical basis, experimental design, and computerized simulation of synergism and antagonism in drug combination studies. *Pharmacol Rev*. 2006;58:621–681.
57. Ley R, Balmanno K, Hadfield K, Weston C, Cook SJ. Activation of the ERK1/2 signaling pathway promotes phosphorylation and proteasome-dependent degradation of the BH3-only protein, Bim. *J Biol Chem*. 2003;278:18811–18816.
58. Luciano F, Jacquel A, Colosetti P, et al. Phosphorylation of Bim-EL by Erk1/2 on serine 69 promotes its degradation via the proteasome pathway and regulates its proapoptotic function. *Oncogene*. 2003;22:6785–6793.
59. Vessey DA, Kelley M, Zhang J, Li L, Tao R, Karliner JS. Dimethylsphingosine and FTY720 inhibit the SK1 form but activate the SK2 form of sphingosine kinase from rat heart. *J Biochem Mol Toxicol*. 2007;21:273–279.
60. Nagaoka Y, Otsuki K, Fujita T, Uesato S. Effects of phosphorylation of immunomodulatory agent FTY720 (Fingolimod) on antiproliferative activity against breast and colon cancer cells. *Biol Pharm Bull*. 2008;31:1177–1181.
61. Roberts KG, Smith AM, McDougall F, et al. Essential requirement for PP2A inhibition by the oncogenic receptor c-KIT suggests PP2A reactivation as a strategy to treat c-KIT+ cancers. *Cancer Res*. 2010;70:5438–5447.
62. Omar HA, Chou CC, Berman-Booty LD, et al. Antitumor effects of OSU-2S, a nonimmunosuppressive analogue of FTY720, in hepatocellular carcinoma. *Hepatology*. 2011;53:1943–1958.